Glycobiology vol. 19 no. 7 pp. 715–725, 2009
doi:10.1093/glycob/cwp039
Advanced Access publication on March 12, 2009

The CMP-legionaminic acid pathway in *Campylobacter*: Biosynthesis involving novel GDP-linked precursors

Ian C Schoenhofen[1], Evgeny Vinogradov, Dennis M Whitfield, Jean-Robert Brisson, and Susan M Logan

Institute for Biological Sciences, National Research Council, Ottawa, Ontario, K1A 0R6 Canada

Received on December 18, 2008; revised on February 17, 2009; accepted on March 7, 2009

The sialic acid-like sugar 5,7-diacetamido-3,5,7,9-tetradeoxy-D-*glycero*-D-*galacto*-nonulosonic acid, or legionaminic acid, is found as a virulence-associated cell-surface glycoconjugate in the Gram-negative bacteria *Legionella pneumophila* and *Campylobacter coli*. *L. pneumophila* serogroup 1 strains, causative agents of Legionnaire's disease, contain an α2,4-linked homopolymer of legionaminic acid within their lipopolysaccharide *O*-chains, whereas the gastrointestinal pathogen *C. coli* modifies its flagellin with this monosaccharide via *O*-linkage. In this work, we have purified and biochemically characterized 11 candidate biosynthetic enzymes from *Campylobacter jejuni*, thereby fully reconstituting the biosynthesis of legionaminic acid and its CMP-activated form, starting from fructose-6-P. This pathway involves unique GDP-linked intermediates, likely providing a cellular mechanism for differentiating between this and similar UDP-linked pathways, such as UDP-2,4-diacetamido-bacillosamine biosynthesis involved in *N*-linked protein glycosylation. Importantly, these findings provide a facile method for efficient large-scale synthesis of legionaminic acid, and since legionaminic acid and sialic acid share the same D-*glycero*-D-*galacto* absolute configuration, this sugar may now be evaluated for its potential as a sialic acid mimic.

Keywords: Campylobacter jejuni/flagellin glycosylation/legionaminic acid/neuraminic acid/sialic acid

Introduction

The sialic acids are a diverse family of α-keto sugars, sharing a defining 9-carbon structural skeleton, and are typically the outermost moiety of oligosaccharides on vertebrate glycolipids and glycoproteins. They are generally attached to the underlying sugar chain via an α-glycosidic linkage between their 2-position (Figure 1) and either the 3- or 6-hydroxyl group of galactose or *N*-acetylgalactosamine, the 6-hydroxyl group of *N*-acetylglucosamine, or they may also exist as α2,8-linked homopolymers (Lehmann et al. 2006). With the presence of various substitutions at their 4, 5, 7, 8, and 9 positions (Varki NM and Varki A 2007), their various linkages, as well as their prominent and accessible location, it is not surprising that this diverse family of sugars mediates and/or modulates a multitude of cellular interactions. Intercellular adhesion and signaling often results from sialic acid-specific binding proteins, or lectins, present on mammalian cell surfaces, most noted for their importance in regulating the immune system and in neuronal development. For example, the Siglecs (*S*ia-recognizing *Ig*-superfamily *lec*tins) MAG and CD22 are involved in the binding of glial cells to gangliosides, which is critical to the long-term stability of myelin as well as inhibition of neurite outgrowth, and in negatively regulating B-cell function, respectively (Varki and Angata 2006; Crocker et al. 2007; Varki 2007). In addition, the neural cell adhesion molecule (NCAM) possesses α2,8-linked polysialic acid, which is important for brain development and neural regeneration, while its expression correlates with poor prognosis for several neuroendocrine tumors (Bork et al. 2007). Another example of sialic acid having prognostic significance in human cancer is the enhanced expression of α2,6-linked sialic acid on *N*-glycans, correlating with cancer progression, metastatic spread and poor prognosis for colon, breast, and cervical cancers, to name a few (Hedlund et al. 2008).

It is possible that the importance of sialic acids within humans has contributed to the abundance of pathogens that display, bind, or catabolize sialic acid. In fact, sialic acids are now recognized as the receptor or ligand most frequently used by pathogenic viruses, bacteria, and protozoa (Lehmann et al. 2006). Furthermore, pathogenic bacteria have gained the ability to display sialic acids on their surface, either by de novo synthesis or through specific scavenging mechanisms, which is believed to influence pathogenesis through immune evasion, adhesion, and invasion (Hsu et al. 2006; Severi et al. 2007). For example, the polysialic acid capsules of *Neisseria meningitidis* B and *Escherichia coli* K1 are poorly immunogenic, likely due to their molecular mimicry with the polysialic acid found on NCAM. In addition to utilizing host sialic acids as nutrient sources, many pathogenic bacteria possess sialic acid-specific lectins, which assist host–pathogen interactions and ultimately pathogenesis. Interestingly, they may also deploy soluble lectins, or toxins, that bind sialoglycoconjugates, such as the AB_5 cholera toxin that recognizes the GM1 ganglioside (Angström et al. 1994; Merritt et al. 1998) and pertussis toxin that recognizes the GD1a ganglioside (Hausman and Burns 1993; Stein et al. 1994). Finally, an increasing number of protozoal pathogens have been found to utilize sialic acid-specific lectins, such as *Plasmodium* spp., the causative agent of malaria (Lehmann et al. 2006). Moreover, Trypanosomes possess a cell-surface trans-sialidase allowing these organisms to coat themselves with mammalian-derived sialic acid (Pontes de Carvalho et al. 1993).

In addition to presenting sialic acids on their surface, bacteria can also incorporate sialic acid-like sugars

[1]To whom correspondence should be addressed: Tel: +1-613-991-2141; Fax: +1-613-952-9092; e-mail: ian.schoenhofen@nrc-cnrc.gc.ca

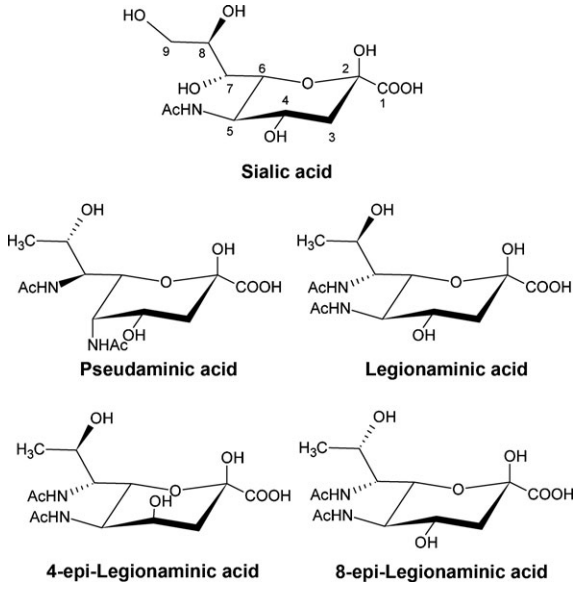

Fig. 1. Structures of sialic acid and sialic acid-like sugars. Sialic acid (Neu5Ac; D-*glycero*-D-*galacto* configuration), pseudaminic acid (Pse5Ac7Ac; L-*glycero*-L-*manno* configuration), legionaminic acid (Leg5Ac7Ac; D-*glycero*-D-*galacto* configuration), 4-epi-legionaminic acid (4eLeg5Ac7Ac; D-*glycero*-D-*talo* configuration), and 8-epi-legionaminic acid (8eLeg5Ac7Ac; L-*glycero*-D-*galacto* configuration) are shown. The thermodynamically more stable anomers, with equatorial carboxyl groups, are depicted. For reference, the nine carbon atoms of sialic acid are numbered.

(5,7-diacetamido-3,5,7,9-tetradeoxy-nonulosonate derivatives) into their virulence-associated cell-surface glycoconjugates, such as lipopolysaccharide (LPS) (Knirel et al. 2003), capsular polysaccharide (Kiss et al. 2001), pili (Castric et al. 2001), and flagella (Thibault et al. 2001; Schirm et al. 2003). These sugars (Figure 1) are unique to microorganisms and may exhibit configurational differences compared with sialic acid. One particular sialic acid-like sugar, legionaminic acid (5,7-diacetamido-3,5,7,9-tetradeoxy-D-*glycero*-D-*galacto*-nonulosonic acid), has the same absolute configuration as sialic acid. It was first identified in 1994 to be a component of *Legionella pneumophila* serogroup 1 LPS, hence its name (Knirel et al. 1994). However, it was not until 2001 that its correct stereochemistry was determined by total synthesis (Tsvetkov et al. 2001). *L. pneumophila*, the causative agent of Legionnaires' disease, invades and replicates within alveolar macrophages leading to a debilitating and sometimes fatal pneumonia (Kooistra et al. 2002). The role of legionaminic acid in this disease progression may be significant, as it has been suggested that LPS is a key determinant in the ability of *L. pneumophila* to inhibit the fusion of phagosomes with lysosomes (Fernandez-Moreira et al. 2006). *L. pneumophila* serogroup 1 LPS contains both legionaminic acid and its 4-epimer isomer (Figure 1), although the majority appears to be an α2,4-linked homopolymer of legionaminic acid (Knirel et al. 2003). Interestingly, the first report of a glycoprotein containing legionaminic acid was the recent discovery of novel legionaminic acid derivatives, *O*-linked to Ser/Thr, on the flagellins of *Campylobacter coli*, a gastrointestinal pathogen (McNally et al. 2007). Here, a number of *Campylobacter* genes (*ptmA-H*) were identified as being critical to their synthesis by screening isogenic mutants for the presence of CMP-legionaminic acid metabolites.

The importance of legionaminic acid as a virulence factor, and its potential in applications as a sialic acid analog, prompted us to elucidate its complete biosynthetic pathway using enzymes from *C. jejuni* 11168 (Figure 2).

Results and discussion

The rationale

As with our characterization of the pseudaminic acid pathway in *Campylobacter* (Schoenhofen, McNally, Brisson, et al. 2006; Figure 1), the elucidation of the legionaminic acid pathway within *Campylobacter* relied heavily on a "holistic" approach involving bioinformatic, comparative genomic, metabolomic, and functional analyses. For clarity in understanding the enzyme function associated with various Cj gene designations and the relationship with previous gene nomenclature, we have tabulated this information as a useful reference (see supplementary Table S1). In addition, we have provided, and are recommending the alternate gene designations to better reflect their roles in CMP-legionaminic acid biosynthesis.

One of the most significant insights was the consideration that this pathway may involve alternative nucleotide-linked intermediates. As it has been documented that different nucleotides within NDP-sugars may allow for the separation of biosynthetic pathways (Nikaido et al. 1966; Ginsburg 1978; Maki and Renkonen 2004) and importantly may provide a means for their independent control and regulation, it was believed that the legionaminic acid pathway within *Campylobacter* may be selective for NDPs other than UDP. This would facilitate its separation from similar UDP-utilizing pathways found in *Campylobacter*, such as those for pseudaminic acid and 2,4-diacetamidobacillosamine, involved in flagellin *O*-linked glycosylation and protein *N*-linked glycosylation, respectively (Figure 3). Several initial findings collectively supported this hypothesis and are as follows. First, Cj1329 (PtmE), a member of the *Campylobacter* flagellin glycosylation locus (Cj1293–Cj1344), was found to exhibit sequence similarity to NDP-sugar pyrophosphorylases or nucleotidyltransferases and in particular, possesses motifs similar to the characteristic activator (G-X-G-T-R-X_2-P-X-T) and sugar (E-E-K-P) binding domains found within NDP-glucose pyrophosphorylases (Silva et al. 2005). In addition to the expected pathway components Cj1328, Cj1327, and Cj1331 (NeuC, B, and A homologs; LegG, LegI, and LegF, respectively), the gene products Cj1329, Cj1330, and Cj1332 (PtmE, PtmF, and PtmA, respectively) were also found to be necessary for the accumulation of CMP-legionaminic acid (XI) in the metabolome of *C. coli* (McNally et al. 2007). The requirement of a possible nucleotidyltransferase (PtmE) supported our hypothesis, in that this enzyme could be responsible for the production of a novel NDP-sugar precursor required for legionaminic acid synthesis. As these enzymes act on NTP donors and sugar-1-P acceptors to form pyrophosphate and NDP-sugars, it was also possible that some members of the Cj1293–Cj1344 locus may be responsible for the production of a sugar-1-P acceptor. PtmA (Cj1332) and PtmF (Cj1330) are annotated as possible oxidoreductases, but upon closer examination we found that they shared limited sequence similarity with the N-terminal glutaminase and C-terminal isomerase domains, respectively, of

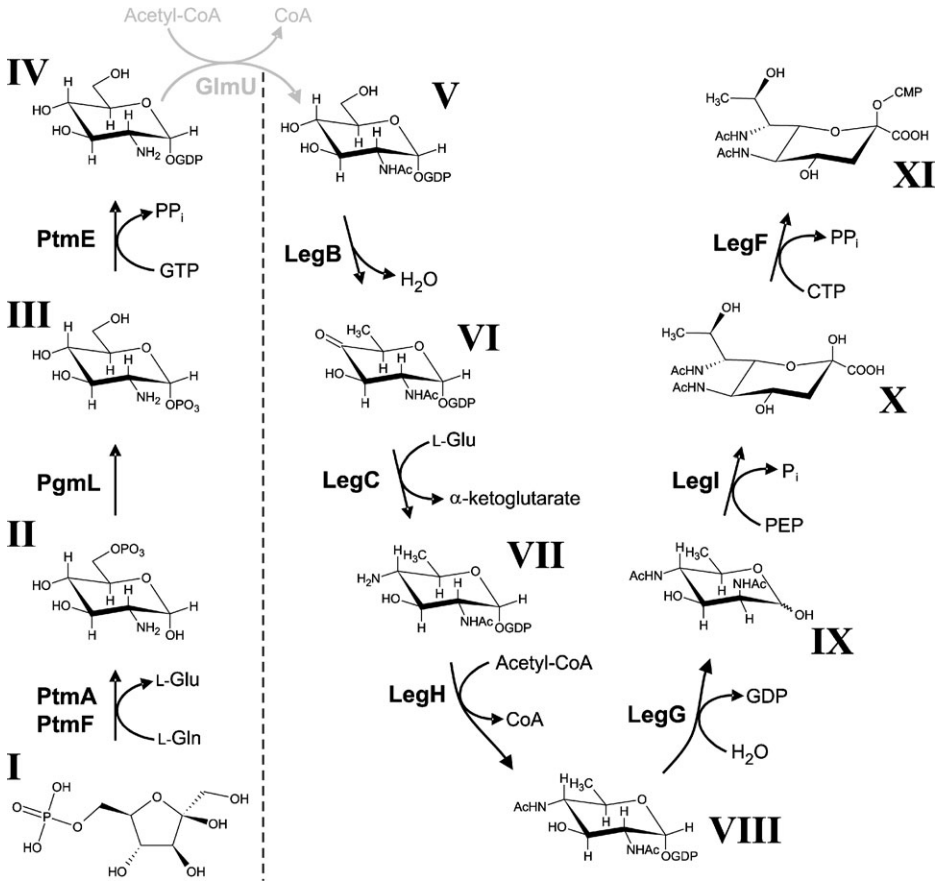

Fig. 2. The CMP-legionaminic acid biosynthetic pathway in *C. jejuni*. This biosynthetic pathway involves two segments: (1) synthesis of a GDP-sugar building block (left of the dashed line) and (2) synthesis of the final CMP-nonulosonate (right of the dashed line), which are linked by the enzymatic step shown in gray. The enzymes and biosynthetic intermediates of the CMP-legionaminic acid pathway in order are PtmA and PtmF, glutaminase and isomerase, respectively, comprising a GlcN-6-P synthase; PgmL, phosphoglucosamine mutase; PtmE, GlcN-1-P guanylyltransferase; GlmU, *N*-acetyltransferase; LegB, NAD-dependent 4,6-dehydratase; LegC, PLP-dependent aminotransferase; LegH, *N*-acetyltransferase; LegG, NDP-sugar hydrolase/2-epimerase; LegI, legionaminic acid synthase; LegF, CMP-legionaminic acid synthetase; and (I) Fru-6-P; (II) GlcN-6-P; (III) GlcN-1-P; (IV) GDP-GlcN; (V) GDP-GlcNAc; (VI) GDP-2-acetamido-2,6-dideoxy-α-D-*xylo*-hexos-4-ulose; (VII) GDP-4-amino-4,6-dideoxy-α-D-GlcNAc; (VIII) GDP-2,4-diacetamido-2,4,6-trideoxy-α-D-glucopyranose; (IX) 2,4-diacetamido-2,4,6-trideoxy-D-mannopyranose; (X) legionaminic acid; (XI) CMP-legionaminic acid. The assignment of roman numerals to each compound is consistent with label designations found throughout the text. For simplicity, all the sugars are shown in $^4C_1$ form, except for the nonulosonates and Fru-6-P.

glucosamine-6-P synthase (GlcN-6-P synthase or GlmS). GlcN-6-P synthase is a key enzyme of hexosamine metabolism and is one of the enzymes responsible for the production of GlcN-1-P or GlcNAc-1-P (Mouilleron et al. 2006). Specifically, PtmA and PtmF were each found to share approximately 40% identity and 60% similarity over only 26 residues with the respective domains of *E. coli* GlcN-6-P synthase. This was surprising as, to date, prokaryotic and eukaryotic GlcN-6-P synthases contain both of these domains within one polypeptide. Further support for our hypothesis that this pathway is selective for NDPs other than UDP was provided by the apparent inability of putative legionaminic acid biosynthetic enzymes to efficiently utilize candidate UDP-sugar precursors. Consequently, very limited biosynthetic yields of XI were obtained when using the *Campylobacter* NeuC, B, and A homologs (LegG, LegI, and LegF) with the UDP-linked intermediate UDP-2,4-diacetamidobacillosamine, or UDP-2,4-diNAc-6-deoxy-Glc, involved in *N*-linked protein glycosylation (data not shown; see Figure 3). Interestingly, Glaze et al. (2008) recently reported similar difficulties, i.e., poor yields of XI, when using the same UDP-linked intermediate with NeuC, B, and A homologs from *L. pneumophila*. The remainder of this article will discuss our findings from in vitro functional analyses of 11 recombinantly produced and affinity-purified enzymes from *C. jejuni* 11168 (Figure 4).

GDP-glucosamine biosynthesis

Further evidence that PtmF and PtmA function in tandem as a GlcN-6-P synthase was the observed stabilization of PtmF by copurification with PtmA. Attempts to isolate only PtmF resulted in aggregates that were unable to enter 12.5% SDS–polyacrylamide gels (data not shown). When PtmF and PtmA were copurified, the PtmF peptide still appeared to aggregate, as indicated by the presence of an additional higher molecular weight species by sodium dodecyl sulfate–polyacrylamide gel electrophoresis (SDS–PAGE) (Figure 4), although to a much lesser extent. As deduced from ^{1}H NMR, PtmF and PtmA were found to efficiently convert fructose-6-P (I) to glucosamine-6-P (II) or glucose-6-P depending on the presence or absence of L-glutamine, respectively (data not shown). These observations

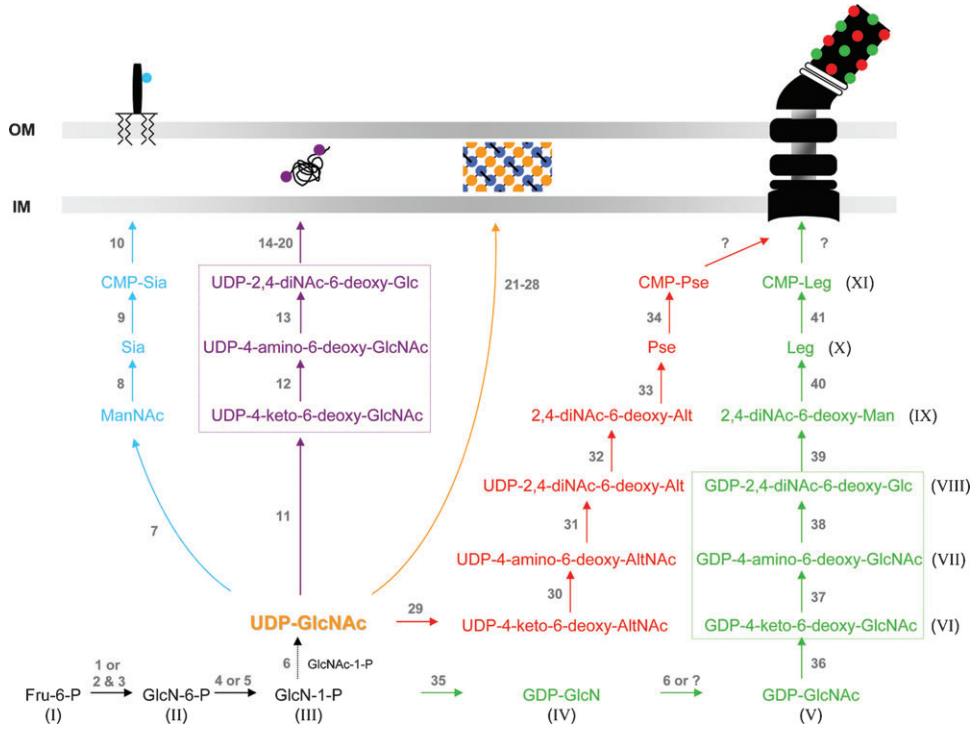

Fig. 3. A selection of extracytoplasmic sugar modifications from the *Campylobacter* cell. Glycosylated structures represented are lipooligosaccharide (cyan), periplasmic *N*-linked glycoproteins (purple), peptidoglycan (orange and blue), and flagella – a polymer of *O*-linked flagellin glycoproteins (green and red). Sugars found within boxes differ only by their nucleotide adduct, a likely discriminatory tool for these glycosylation pathways. Note that glycosyltransferases responsible for *O*-glycan attachment to flagellin have yet to be identified. Roman numeral designations are consistent with those found throughout the text and refer to the CMP-legionaminic acid intermediates identified in this study. The enzymes (gray numbers) and alternate sugar names are found in supplementary Tables S2 and S3, respectively.

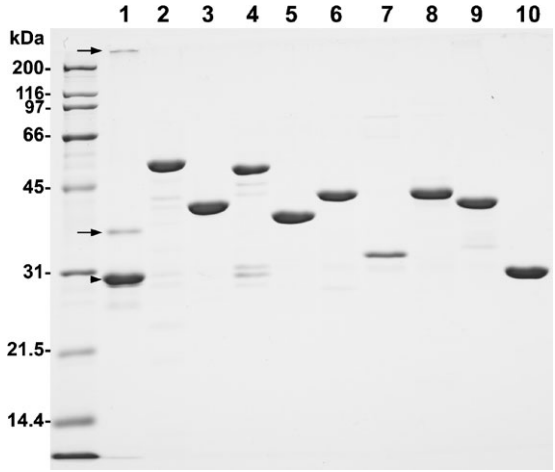

Fig. 4. Sodium dodecyl sulfate-polyacrylamide gel electrophoresis (12.5%) analyses of CMP-legionaminic acid biosynthetic enzymes from *Campylobacter jejuni* 11168 after nickel-nitrilotriacetic acid purification. Lane 1, PtmAHis$_6$ (arrowhead) and His$_6$PtmF (arrow); lane 2, PgmLHis$_6$; lane 3, His$_6$PtmE; lane 4, His$_6$GlmU; lane 5, LegBHis$_6$; lane 6, His$_6$LegC; lane 7, His$_6$LegH; lane 8, His$_6$LegG; lane 9, His$_6$LegI; lane 10, LegFHis$_6$. Molecular mass standards are shown on the left in kDa.

are similar to findings reported for other GlcN-6-P synthases (Teplyakov et al. 1999). To our knowledge, this is the first report of a GlcN-6-P synthase whose functional domains, glutaminase and isomerase, are not naturally fused, the significance of which is currently unknown.

The next committed step in bacterial hexosamine biosynthesis would involve conversion of II to glucosamine-1-P (III) by a phosphoglucosamine mutase. The appropriate mutase was unclear, and as such, we had to look outside of the flagellar glycosylation locus. As the GlcN-6-P synthase is the rate-limiting enzyme in hexosamine metabolism (Mouilleron et al. 2006), it was believed that a general "house-keeping" mutase might be sufficient enough to perform the necessary interconversions for flagellin glycosylation. Originally, Cj0360, an annotated GlmM mutase, was tested and appeared to accumulate GlcN-1,6-diP from II as deduced using ^{1}H NMR (data not shown), but not GlcN-1-P (III). Surprisingly, the gene Cj1407c was also annotated as a phosphoglucomutase and is juxtaposed to *fliL* (Cj1408), a flagellar component that localizes to the cytoplasmic face of the flagellar basal body MS ring in *Campylobacter*. Cj1407c, now annotated as PgmL for its involvement in the legionaminic acid pathway, catalyzed the interconversion of II to III without the exogenous addition of Glc-1,6-diP or GlcN-1,6-diP that is typically required for GlmM enzymes (Mengin-Lecreulx and van Heijenoort 1996; Jolly et al. 1999) and allowed for a "one-pot" enzymatic synthesis of GDP-GlcN (IV; see below). PgmL was also capable of converting Glc-6-P to Glc-1-P, as evidenced by the accumulation of GDP-Glc, in addition to IV, in GDP-GlcN "one-pot" reactions (see below).

In determining the nucleotide utilized by the legionaminic acid pathway, we initially looked at the specificity of the nucleotidyltransferase. PtmE was found to be absolutely specific for GTP in reactions involving III (supplementary Figure S1). Importantly, this enabled the large-scale production and

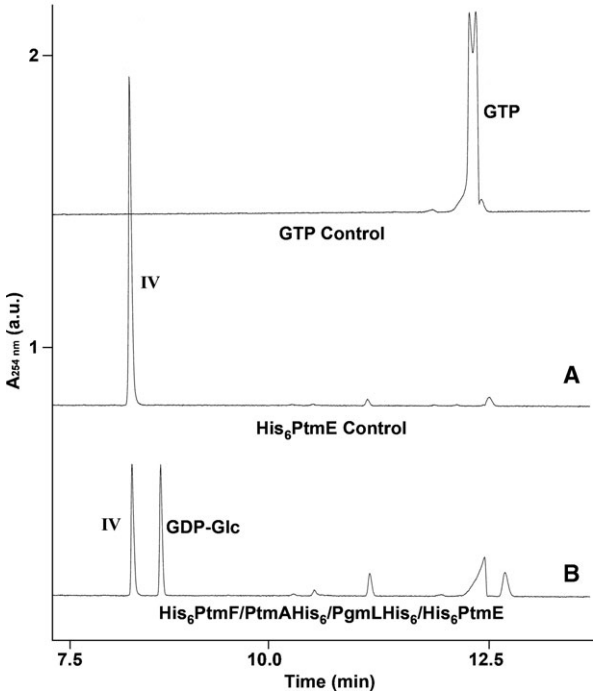

Fig. 5. Capillary electrophoresis analysis of a "one-pot" enzymatic reaction forming GDP-GlcN from Fru-6-P. A control PtmE reaction (**A**) initially contained GlcN-1-P (III), GTP, and His_6PtmE, while the "one-pot" reaction (**B**) contained Fru-6-P (I), GTP, and each of His_6PtmF, PtmAHis_6, Pgm$LHis_6$, and His_6PtmE. The locations of GTP, IV, and GDP-α-D-Glc are also indicated within the figure. *a.u.*, arbitrary units.

purification of IV (Figure 5A and supplementary Table S4). In addition, when using GlcNAc-1-P as a sugar acceptor, PtmE exhibited promiscuity with respect to activator NTP donors (supplementary Figure S1). This allowed for the large-scale production and purification of GDP-GlcNAc (V), CDP-GlcNAc, and TDP-GlcNAc (Table I and supplementary Table S4) for further testing within the pathway. Note that bacterial cells accumulate III instead of GlcNAc-1-P due to the bifunctional nature of the UDP-GlcNAc forming enzyme GlmU (Mengin-Lecreulx and van Heijenoort 1994), in contrast to eukaryotes that accumulate GlcNAc-1-P primarily due to the actions of a glucosamine-6-P *N*-acetyltransferase (Buse et al. 1996). As such, it seemed highly probable that the legionaminic acid pathway may utilize guanine nucleotide precursors since PtmE is absolutely specific for GTP in reactions involving the abundant bacterial hexosamine metabolite GlcN-1-P (III). Ultimately, this was confirmed upon further testing of pathway components (see below). In addition, PtmE exhibited specificity for the C4 configuration of Glc as no activity was observed when using GalN-1-P, but activity was observed with Glc-1-P (see below), GlcN-1-P, and GlcNAc-1-P. Note that *ptmE* contains an additional upstream sequence of unknown function called a CBS domain (originally found in *c*ystathione *b*eta-*s*ynthase), which may be involved at some level of regulation.

The efficiency of these NDP-hexosamine enzymes was demonstrated by the production of IV from a "one-pot" enzymatic reaction involving PtmF, PtmA, PgmL, and PtmE, starting from I (Figure 5). In addition to IV, the accumulation of GDP-Glc was also observed in the "one-pot" reaction, a consequence of PtmF/PtmA producing Glc-6-P upon depletion of L-glutamine as well as promiscuity of the downstream enzymes. The identities of the two products observed in Figure 5B were confirmed by further purification and CE-MS analyses (data not shown), NMR analyses (supplementary Table S4), and comparisons with a control preparation of IV (Figure 5A).

Table I. NMR chemical shifts δ (ppm) for the sugars of compounds **V–XI**

Compound	^{1}H	δ_H (ppm)	^{13}C	δ_C (ppm)
V	H1	5.51	C1	95.1
	H2	3.99	C2	54.5
	H3	3.81	C3	71.7
	H4	3.55	C4	70.3
	H5	3.92	C5	73.8
	H6	3.82/3.86	C6	61.2
VI	H1	5.45	C1	95.3
	H2	4.10	C2	53.5
	H3	3.82	C3	72.4
	H5	4.11	C5	70.9
	H6	1.21	C6	12.4
VII	H1	5.50	C1	95.6
	H2	4.06	C2	55.0
	H3	3.87	C3	69.1
	H4	2.96	C4	58.6
	H5	4.21	C5	68.0
	H6	1.32	C6	18.0
VIII	H1	5.50	C1	95.4
	H2	4.05	C2	55.2
	H3	3.80	C3	69.8
	H4	3.68	C4	57.9
	H5	4.05	C5	69.3
	H6	1.16	C6	18.0
		α/β		α/β
IX	H1	5.11/4.96	C1	94.0/94.0
	H2	4.30/4.46	C2	53.8/54.8
	H3	4.06/3.84	C3	67.7/71.7
	H4	3.77/3.66	C4	54.8/54.5
	H5	3.97/3.51	C5	68.1/72.6
	H6	1.19/1.21	C6	18.0/18.0
X	H3a	1.83	C3	40.8
	H3e	2.22		
	H4	3.96	C4	68.5
	H5	3.72	C5	53.8
	H6	4.24	C6	70.4
	H7	3.86	C7	54.3
	H8	3.86	C8	67.5
	H9	1.16	C9	20.4
XI	H3a	1.63 ($J_{3a,4}$ 11.9; $J_{3a,P}$ 5.8)	C3	42.6
	H3e	2.48 ($J_{3e,4}$ 4.7; $J_{3e,3a}$ 13.4)		
	H4	3.98 ($J_{4,5}$ 10.3)	C4	68.3
	H5	3.72 ($J_{5,6}$ 10.3)	C5	53.7
	H6	4.33 ($J_{6,7}$ 1.5)	C6	72.3
	H7	3.77 ($J_{7,8}$ 9.5)	C7	55.3
	H8	4.03 ($J_{8,9}$ 6.4)	C8	66.9
	H9	1.10	C9	19.5

Conversion of GDP-GlcN to GDP-GlcNAc

As the synthesis of legionaminic acid would be expected to utilize a 2,4-diacetamido-hexose sugar (Schoenhofen, Lunin, et al. 2006), the assumption was that a GDP-HexNAc intermediate fed into the nonulosonate pathway, thereby reducing the number of enzymatic manipulations required, i.e., IV was not the initial nonulosonate building block. This was later confirmed, as the initial nonulosonate pathway enzyme exhibited preference for the *N*-acetyl group of V (see below). Of all the enzymatic manipulations leading to the nonulosonate pathway

precursor V, it is this step in which we are most uncertain. Since the bifunctional UDP-GlcNAc forming enzyme GlmU, which is responsible for the conversion of III to GlcNAc-1-P with subsequent uridylation, is capable of converting UDP-GlcN to UDP-GlcNAc at low efficiencies (Pompeo et al. 2001), we sought to determine if *Campylobacter* GlmU was able to *N*-acetylate IV. This GlmU was found to convert IV to V, but not to completion as is seen with a control *N*-acetylation reaction using its natural substrate III instead of IV (supplementary Figure S2). We are currently screening other putative *N*-acetyltransferases from the flagellar glycosylation locus, such as Cj1296/97, Cj1321, and Cj1322/23, for their ability to catalyze efficient conversion of IV to V. Finally, we feel it is unlikely that the pathway would initially proceed I→II→III→GlcNAc-1-P→V**,** as the promiscuous nature of PtmE with GlcNAc-1-P would result in lowered synthesis of V, but we cannot rule out this possibility. Importantly, our suggested scheme (Figure 2) would also allow PtmE to act on the abundant levels of endogenous III.

Biosynthesis of CMP-legionaminic acid from GDP-GlcNAc

Using the knowledge gained from elucidating the CMP-pseudaminic acid pathway in *Helicobacter pylori* (Schoenhofen, Lunin, et al. 2006; Schoenhofen, McNally, Brisson, et al. 2006; Schoenhofen, McNally, Vinogradov, et al. 2006), we began unraveling the biosynthetic route for CMP-legionaminic acid (XI), the findings of which are summarized in Figure 2 and Table I. Recent metabolomics findings discounted Cj1319 (LegB) and Cj1320 (LegC), the only remaining putative dehydratase and aminotransferase left in the *Campylobacter* flagellar glycosylation locus, as having a role in legionaminic acid synthesis (McNally et al. 2007). In contrast, we found these enzymatic manipulations necessary within this pathway. By examining the ability of LegB to act as a dehydratase, we found it to perform C4,6 dehydration of V (Figure 6). Initial reactions only included V and LegB, but failed. However, as NAD(P)$^+$ is usually tightly coupled to these particular enzymes, since it is a necessary cofactor for the C4,6 dehydratase reaction, we added NAD$^+$ and NADP$^+$ exogenously in separate reactions. In doing so, LegB was found to catalyze the efficient turnover of V in an NAD$^+$-dependent manner forming the product GDP-2-acetamido-2,6-dideoxy-α-D-*xylo*-hexos-4-ulose (VI; Figure 6A). It should be noted that other LegB reactions, in the presence or absence of NAD(P)$^+$, with IV, UDP-GlcNAc, CDP-GlcNAc, TDP-GlcNAc, and TDP-Glc did not yield discernable product (data not shown). Furthermore, LegC catalyzed the efficient aminotransfer of VI, forming GDP-4-amino-4,6-dideoxy-α-D-GlcNAc (VII) in a PLP-dependent manner (Figure 6B). LegC is specific for the GDP-keto intermediate VI, as it was unable to convert the UDP-keto intermediates from the pseudaminic acid or 2,4-diacetamido-bacillosamine pathways (Figure 3), providing further support for its role in legionaminic acid synthesis. The in vivo metabolomic and in vitro enzymatic discrepancy for LegB/LegC may be explained by possible low-level crosstalk of pathway intermediates within *Campylobacter*. This is further strengthened by our observation that low-levels of XI may be obtained when using the sialic acid homologs LegG (Cj1328), LegI (Cj1327), and LegF (Cj1331) with UDP-2,4-diacetamido-bacillosamine from the *N*-linked glycosylation pathway (data not shown).

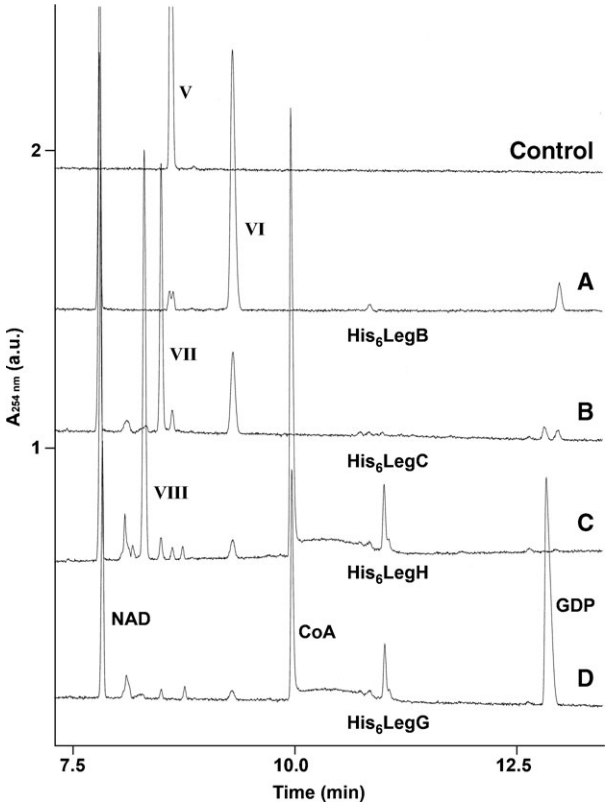

Fig. 6. Capillary electrophoresis analysis of the reaction products obtained after the sequential addition of LegBHis$_6$ (**A**), His$_6$LegC (**B**), His$_6$LegH (**C**), and His$_6$LegG (**D**) to GDP-α-D-GlcNAc. Reactions contained 1 mM GDP-α-D-GlcNAc, 0.5 mM NAD, 0.8 mM PLP, 8 mM L-Glu, and 1.2 mM acetyl-CoA as required. The locations of GDP-α-D-GlcNAc (V), GDP-2-acetamido-2,6-dideoxy-α-D-*xylo*-hexos-4-ulose (VI), GDP-4- amino-4,6-dideoxy-α-D-GlcNAc (VII), GDP- 2,4-diacetamido-2,4,6-trideoxy-α-D-Glc (VIII), NAD, CoA, and GDP are indicated within the figure. *a.u.*, arbitrary units.

The next expected step in the synthesis of XI would involve *N*-acetylation of VII by a respective transferase. As there are several such uncharacterized transferases in the *Campylobacter* flagellin glycosylation locus (Cj1296/97, Cj1298, Cj1321, and Cj1322/23), we initially attempted reactions with PglD, the *N*-acetyltransferase involved in UDP-2,4-diacetamido-bacillosamine biosynthesis (Olivier et al. 2006; Figure 3). The normal substrate of PglD is identical to VII only it is UDP-linked. To our surprise, PglD was able to catalyze *N*-acetyltransfer of VII, forming GDP-2,4-diacetamido-2,4,6-trideoxy-α-D-Glc (VIII) (data not shown). However, the eventual screening of Cj1298 (LegH) exhibited much greater catalytic rates, resulting in 100% conversion of VII to VIII (Figure 6C). This, together with the presence of Cj1298 within the flagellar glycosylation locus, leads us to conclude that LegH is a dedicated component of legionaminic acid biosynthesis. Importantly, this in vitro cross-complementation of LegH function by PglD may have prevented its initial identification from in vivo metabolomics screening.

Likely, the most critical checkpoint between the *N*-linked protein glycosylation and legionaminic acid pathways within *Campylobacter* is the reaction catalyzed by the NeuC homolog, LegG. This enzyme is expected to perform a C2

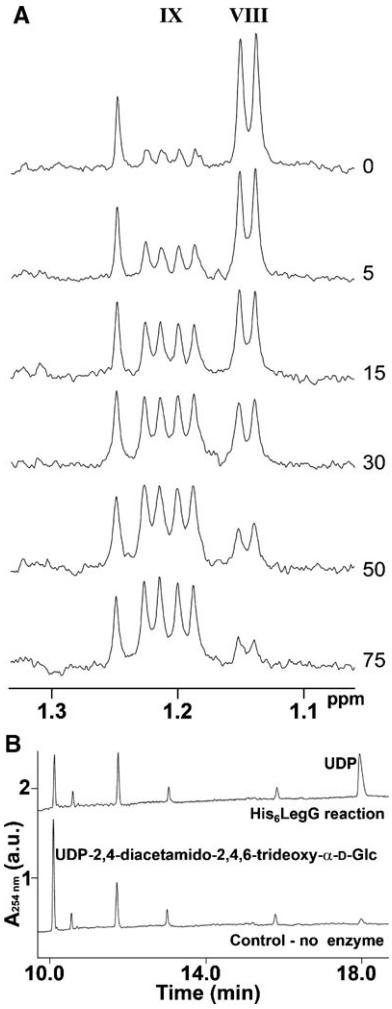

Fig. 7. Kinetics and substrate specificity of His_6LegG. (**A**) The His_6LegG reaction with GDP-2,4-diacetamido-2,4,6-trideoxy-α-D-Glc (VIII) monitored directly with ^{1}H NMR spectroscopy. ^{1}H NMR spectra were acquired over time (min) as indicated, and the C-6 CH_3 proton region of substrate (VIII) and product (IX) is shown. (**B**) Capillary electrophoresis analysis of the His_6LegG reaction with UDP-2,4-diacetamido-2,4,6-trideoxy-α-D-Glc after incubation for 90 min at 37°C and then 16 h at 25°C, using ~10-fold more enzyme than in **A**. The locations of UDP and UDP-2,4-diacetamido-2,4,6-trideoxy-α-D-Glc are indicated within the figure, where a.u. is arbitrary units.

epimerization resulting in NDP removal, and in fact, LegG was found to efficiently remove the NDP from substrate VIII (Figure 6D). Upon examination of the sugar product formed, by performing "in-tube" NMR reactions, we observed efficient catalysis of VIII, such that the formation of 2,4-diacetamido-2,4,6-trideoxy-D-Man (IX) was near completion within 75 min using only 4 μg of LegG (Figure 7A). Using similar conditions, IX was not observed when the natural product of PglD, UDP-2,4-diacetamido-2,4,6-trideoxy-α-D-Glc (Figure 3), was used as a substrate. Although, when we increased the quantity of LegG 10-fold within this reaction, UDP removal was observed (Figure 7B), but product IX was not. Instead, we observed small quantities of 6-deoxy-2,4-diacetamidoglucal (supplementary Figure S3), an unlikely candidate for the next condensation reaction. As we were able to generate small quantities of XI using the UDP-linked intermediate above, it is possible that the glucal product or nondetectable quantities of IX may inefficiently condense with pyruvate in the next enzymatic step. However, we conclude that the natural synthetic route is as summarized in Figure 2. Note that LegG was also found to catalyze turnover of V with moderate efficiency as assessed by CE (data not shown), which may be an alternative means of accumulating the sialic acid precursor ManNAc within *Campylobacter*. This is the reason why our large-scale biosynthesis of legionaminic acid (X) involved two separate "one-pot" reactions (i.e., V→VIII then VIII→X). Finally, the roles of the NeuB and NeuA homologs LegI (Cj1327) and LegF (Cj1331), respectively, were confirmed. LegI catalyzed the condensation of IX with pyruvate to form X, while LegF efficiently CMP-activated X (Table I).

Conclusions

In summary, we have outlined a facile method for the enzymatic preparation (mg to g quantities) of CMP-legionaminic acid (Figure 8), and corresponding pathway intermediates. As synthetic yields obtained from chemical methods are low, only 7% from condensation of IX with oxaloacetic acid (Tsvetkov et al. 2001), our enzymatic method provides an attractive synthetic alternative. Also, since we have defined the NDP-hexosamine enzymatic steps from I, the engineering of *E. coli* producing strains is now possible (Lundgren and Boddy 2007), with production efficiencies predicted to far-surpass those from in vitro enzymatic methods. The legionaminic acid biosynthetic route described is similar to that proposed by Schoenhofen, Lunin, et al. (2006) and Glaze et al. (2008), except that the sugar precursors are GDP-linked rather than UDP-linked. This likely assists the regulation of *O*-linked flagellin glycosylation and *N*-linked protein glycosylation pathways (Figure 3) within *Campylobacter*, as these pathways may tap into unique metabolite pools. Aside from utilizing different nucleotides, the biosynthetic routes for pseudaminic acid and legionaminic acid differ in the epimerizations performed at C2, C4, and C5 of the 6-deoxy-hexose intermediates, resulting in stereo-chemical differences at C5, C7, and C8 of the final nonulosonates.

Importantly, legionaminic acid shares the same D-*glycero*-D-*galacto* absolute configuration as sialic acid. Aside from the suggested role of sialic acid-like sugars to protect *Campylobacter* cells from host defenses by subverting the host complement pathway, the potential interaction of these sugars with host sialic acid-specific lectins may explain their possible influence in adhesion and infection. This would be in addition to the previously reported roles of *Campylobacter* lipo-oligosaccharyl sialylated glycans in facilitating cell adhesion through interactions with Siglec-7 (Avril et al. 2006). It is also tempting to speculate that legionaminic acid on the surface of *L. pneumophila* may be the critical factor responsible for inhibiting phagosome–lysosome fusion within macrophages (Fernandez-Moreira et al. 2006), possibly by interfering with the macrophage sialic-acid-dependent adhesion molecule, sialoadhesin. In support of this hypothesis, a recent genomic study implicated the LPS of *L. pneumophila* serogroup 1 as a conserved determinant in the ability to cause human disease (Cazalet et al. 2008). Serogroup 1 strains are the principal cause of human legionellosis disease, being responsible for approximately 84% of all cases worldwide (Yu et al. 2002). In addition, a similar scenario has been reported for the porcine virus PRRSV, where

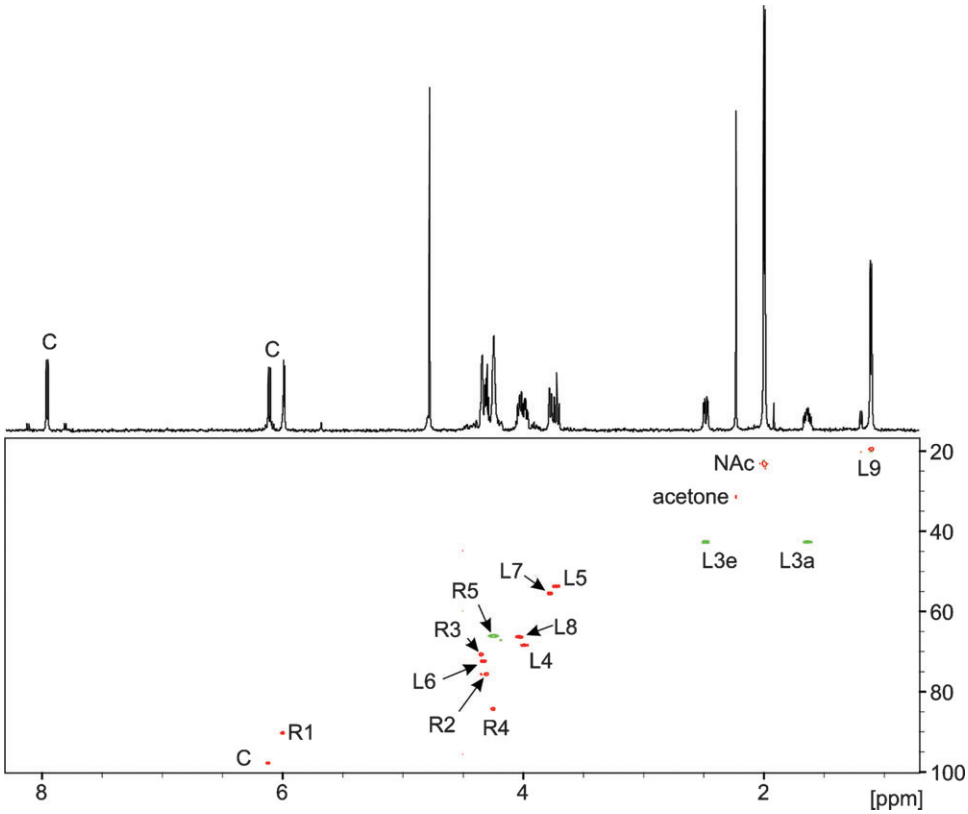

Fig. 8. The ^{1}H spectrum and ^{1}H-^{13}C HSQC correlation spectrum of CMP-legionaminic acid (XI). Spectra were recorded on a Varian Inova Unity 500 MHz spectrometer with standard Varian pulse sequences in D_2O at 25°C, with 4 scans for the ^{1}H spectrum and 32 scans for HSQC. C, cytosine; R, ribose; L, legionaminic acid; NAc, 5-NHAc and 7-NHAc CH3 regions of legionaminic acid; and acetone was included as an internal reference.

it was recently found to exploit the sialic acid binding properties of sialoadhesin for attachment and infection (Delputte et al. 2007). Due to the pathogenic importance of *L. pneumophila* LPS, the enzymatic pathway outlined in this study may be used to assist the identification and development of therapeutics to treat *L. pneumophila* infections. Of great significance, the methods developed in this study may now be harnessed to investigate the potential of legionaminic acid within sialo-biology applications.

Material and methods

His$_6$-tagged protein expression and purification

Plasmid DNA construction and sequencing were similar to previously described methods (Schoenhofen, McNally, Brisson, et al. 2006; Schoenhofen, McNally, Vinogradov, et al. 2006). Vector or recombinant plasmids were transformed by electroporation into electrocompetent Top10F′ or DH10B (Invitrogen, Burlington, ON) *Escherichia coli* cells for cloning purposes or BL21[DE3] (Novagen, Gibbstown, NJ) *E. coli* cells for protein production, except for the expression clone pNRC51.1 which was electroporated into BL21-CodonPlus[DE3]-RIL (Novagen, Gibbstown, NJ) *E. coli* cells. PCR was used to amplify *Campylobacter jejuni* 11168 DNA for subsequent cloning. A list of cloning vectors and recombinant plasmids is provided in supplementary Table S5, and pertinent oligonucleotides are provided in supplementary Table S6. Newly constructed plasmids are as follows: pNRC145.3, encoding an N-terminal His$_6$-tagged derivative of Cj1330 or PtmF; pNRC141.1, encoding a C-terminal His$_6$-tagged derivative of Cj1332 or PtmA; pNRC173.1, encoding a C-terminal His$_6$-tagged derivative of Cj1407c or PgmL; pNRC136.1, encoding an N-terminal His$_6$-tagged derivative of Cj1329 or PtmE; pNRC175.1, encoding an N-terminal His$_6$-tagged derivative of Cj0821 or GlmU; pNRC16.1, encoding a C-terminal His$_6$-tagged derivative of Cj1319 or LegB; pNRC83.1, encoding an N-terminal His$_6$-tagged derivative of Cj1320 or LegC; pNRC164.3, encoding an N-terminal His$_6$-tagged derivative of Cj1298 or LegH; pNRC134.1, encoding an N-terminal His$_6$-tagged derivative of Cj1328 or LegG; pNRC51.1, encoding an N-terminal His$_6$-tagged derivative of Cj1327 or LegI; and pNRC139.1, encoding a C-terminal His$_6$-tagged derivative of Cj1331 or LegF.

Typically, each expression strain was grown in 1–2 L of 2× yeast tryptone (Schoenhofen, McNally, Vinogradov, et al. 2006), depending on the expression level, with either kanamycin (50 μg mL^{-1}) and ampicillin (75 μg mL^{-1}) or ampicillin and chloramphenicol (100 μg mL^{-1} and 40 μg mL^{-1}) for selection. The cultures were grown at 30°C, induced at an OD_{600} of 0.6 with 0.1 mM isopropyl-1-thio-β-D-galactopyranoside, and harvested 2.75 h later. For the "GDP-hexosamine" biosynthetic enzymes (PtmF, PtmA, PgmL, and PtmE), cell pellets were resuspended in the lysis buffer (25 mM Tris, pH 7.5, 400 mM NaCl, 10 mM β-mercaptoethanol) containing 10 mM imidazole and complete protease inhibitor mixture, EDTA-free

(Roche Applied Science, Laval, QC). After the addition of 10 μg mL^{-1} of DNaseI (Roche Applied Science, Laval, QC), the cells were disrupted by two passes through an emulsiflex C5 (20,000 psi). Lysates were centrifuged at 100,000 × *g* for 50 min at 4°C, and the supernatant fraction was applied to a 2 mL nickel-nitrilotriacetic acid (Qiagen, Mississauga, ON) column equilibrated in the 10 mM imidazole lysis buffer, using a flow rate of 1 mL min^{-1}. After sample application, the column was washed with 10 column volumes of 10 mM imidazole lysis buffer. To elute the protein of interest, a linear gradient from 10 to 100 mM imidazole, in the lysis buffer, over 25 column volumes was applied to the column prior to a final pulse of 20 column volumes of 200 mM imidazole lysis buffer. Fractions containing the purified protein of interest, as determined by SDS–PAGE (12.5%) and Coomassie staining, were pooled and dialyzed against the dialysis buffer (25 mM Tris, pH 7.5) overnight at 4°C. When purifying PtmE for the "large-scale" production of NDP-sugars, the dialysis buffer contained 50 mM Tris, pH 7.5. In addition, PtmF and PtmA were purified together by combining respective resuspended cell pellets before cell lysis. For the "nonulosonate" biosynthetic enzymes (LegB, LegC, LegH, LegG, LegI, and LegF) and GlmU, purification was similar to that mentioned above, except that the lysis buffer contained 50 mM sodium phosphate instead of Tris and the dialysis buffer consisted of 25 mM sodium phosphate, 25 mM NaCl. The pH was adjusted from 7.3 to 7.8 depending on the theoretical pI of each protein. Furthermore, the dialysis buffer for GlmU additionally contained 10 mM β-mercaptoethanol. Protein concentration was measured spectrophotometrically using A_{280} 0.1% values ($PgmLHis_6$, 0.693; His_6PtmE, 0.513; His_6GlmU, 0.517; $LegBHis_6$, 0.892; His_6LegC, 0.625; His_6LegH, 1.06; His_6LegG, 0.432; His_6LegI, 0.242; $LegFHis_6$, 0.385; and protein concentration was estimated for $His_6PtmF/PtmAHis_6$ preparations using an averaged 0.1% value of 0.82). Yields of purified protein were typically 20 mg L^{-1} of cell culture, except for His_6LegC, His_6LegH, and His_6LegI with yields of 6, 2.5, and 7.5 mg L^{-1} of cell culture, respectively.

Enzymatic reactions and metabolite purification

Enzymatic reactions were performed for 4.5 h at 37°C and then overnight at 25°C, with approximately 200 μg mL^{-1} respective protein concentration using chemicals from Sigma (Oakville, ON) unless otherwise indicated.

GDP-Glucosamine Biosynthesis. The "one-pot" enzymatic synthesis of GDP-GlcN from Fru-6-P (I→IV) was accomplished using a 3 mL reaction containing His_6PtmF, $PtmAHis_6$, $PgmLHis_6$, His_6PtmE, 5 mM Fru-6-P (I), 10 mM L-Gln, 1 mM DTT, 5 mM $MgCl_2$, 0.8 U mL^{-1} pyrophosphatase, and 2.5 mM GTP in 25 mM Tris, pH 7.5. Large-scale enzymatic synthesis of GDP-GlcN (IV) was accomplished using a 12 mL reaction containing 50 mM Tris, pH 7.5, 1 mM GTP, 1 mM $MgCl_2$, 0.8 U mL^{-1} pyrophosphatase, 1.2 mM GlcN-1-P (III), and approximately 4.8 mg of His_6PtmE. The large-scale enzymatic synthesis of GDP-GlcNAc (V) was performed similar to that discussed above, except that the scale was increased 5-fold and GlcNAc-1-P was used in place of GlcN-1-P. Assessment of His_6PtmE substrate specificity was accomplished using nine reactions, 80 μL each, containing 50 mM Tris, pH 7.5, 2 mM $MgCl_2$, 50 μg of His_6PtmE, and various combinations of 10 mM sugar-1-P (GalN-1-P, GlcN-1-P, or GlcNAc-1-P), and 0.2 mM NTP (CTP, GTP, or TTP).

Conversion of GDP-GlcN to GDP-GlcNAc. The His_6GlmU reaction was performed using 1 mM GDP-GlcN (IV), 1.2 mM acetyl-CoA, and His_6GlmU in 25 mM sodium phosphate, pH 7.8, 25 mM NaCl, and 10 mM β-mercaptoethanol. In addition, a control reaction was performed containing 1 mM GlcN-1-P (III) instead of IV.

Biosynthesis of Legionaminic Acid from GDP-GlcNAc. The stepwise enzymatic synthesis of intermediates or products was accomplished in two stages (V→VI→VII→VIII, and then VIII→IX→X) using 1 mM of V, 0.5 mM NAD, 0.8 mM PLP, 8 mM L-Glu, 1.2 mM acetyl-CoA, 1.2 mM PEP, $LegBHis_6$, His_6LegC, His_6LegH, His_6LegG, and His_6LegI as appropriate, in 25 mM sodium phosphate, pH 7.3, 25 mM NaCl. Assessment of His_6LegG activity involved in monitoring the reaction kinetics by ^1H NMR (see NMR spectroscopy) for 75 min using 0.75 mM GDP-2,4-diacetamido-2,4,6-trideoxy-α-D-Glc (VIII), 4 μg of His_6LegG in 200 μL of 25 mM sodium phosphate, pH 7.3, 25 mM NaCl at 25°C. In addition, the substrate flexibility of His_6LegG was assessed using a 300 μL reaction containing 40 μg of His_6LegG, 25 mM sodium phosphate, pH 7.3, 25 mM NaCl, and 0.75 mM UDP-2,4-diacetamido-2,4,6-trideoxy-α-D-Glc, with incubation at 37°C for 1.5 h and then overnight at 25°C.

Biosynthesis of CMP-legionaminic Acid. The CMP-activation of legionaminic acid (X→XI) was performed using a 20 mL reaction containing approximately 0.2 mM of X, 50 mM $MgCl_2$, 3 mM CTP, and 15 mg of $LegFHis_6$ in 25 mM sodium phosphate, pH 7.8, 25 mM NaCl, with incubation at 37°C for 5 h and then 25°C for 72 h.

Metabolite Purification. Typically, reactions were passed through an Amicon Ultra-15 (10,000 molecular weight cutoff) or Ultra-4 (5000 molecular weight cutoff) filter membrane before analysis. As required, NDP-sugar preparations (GDP-Glc, GDP-GlcN, GDP-GlcNAc, CDP-GlcNAc, TDP-GlcNAc, and CMP-Leg) were lyophilized and desalted/purified using a Superdex Peptide 10/300 GL (GE Healthcare, Piscataway, NJ) column in 25 mM ammonium bicarbonate, pH 7.9. For further purity, the above-mentioned NDP-sugar samples were subjected to anion-exchange chromatography (Mono Q 4.6/100 PE, GE Healthcare, Piscataway, NJ) using ammonium bicarbonate, pH 7.9. Quantification of NDP-sugar preparations was determined using the molar extinction coefficients of CMP (ε_{260} = 7400), GDP (ε_{260} = 11,500), TDP (ε_{260} = 8700), and UDP (ε_{260} = 10,000).

CE and CE-MS analysis

CE analysis was performed using either a P/ACE 5510 or P/ACE MDQ system (Beckman Instruments, Mississauga, ON) with diode array detection. The capillaries were bare silica 50 μm × 50 cm, with a detector at 50 cm, and the running buffer was 25 mM sodium tetraborate, pH 9.4. Samples were introduced by pressure injection for 6 s, and the separation was performed at 18 kV for 20 min. Peak integration was done using the Beckman P/ACE station software.

CE-MS was performed using a Prince CE system (Prince Technologies, Netherlands) coupled to a 4000 QTRAP mass spectrometer (Applied Biosystems/MDS Sciex, Concord, ON). Separations were obtained on an ∼90 cm bare silica capillary using 10 mM ammonium acetate in deionized water, pH 7. A separation voltage of 20 kV, together with a pressure of 500 mbar was used for fast CE-MS analysis. The −5.2 kV electrospray ionization voltage was used for negative-ion mode detection.

NMR spectroscopy

Enzymatic reactions were carried out in 3 mm NMR tubes at 25°C in 10% D_2O and were monitored through the acquisition of the ^1H spectrum at various time intervals (indicated in min) using a Varian Inova 500 MHz (^1H) spectrometer with a Varian Z-gradient 3 mm probe. For structural characterization of compounds, filtered enzymatic reactions or purified material was exchanged into 100% D_2O. Structural analysis was performed using a Varian 600 MHz (^1H) spectrometer with a Varian 5 mm Z-gradient triple resonance cryogenically cooled probe for optimal sensitivity. All spectra were referenced to an internal acetone standard (δ_H 2.225 ppm and δ_C 31.07 ppm).

Acknowledgements

We thank Annie Aubry and Anna Burianova for technical assistance with plasmid construction and growths of expression strains, Denis Brochu for CE technical assistance, Jacek Stupak for CE-MS technical assistance, Dr. David McNally and Nam Khieu for initial NMR characterization, and Tom Devecseri for assistance in preparing figures.

Conflict of interest statement

None declared.

Supplementary Data

Supplementary data for this article is available online at http://glycob.oxfordjournals.org/.

Abbreviations

4-epi-legionaminic acid (4eLeg5Ac7Ac), 5,7-diacetamido-3,5,7,9-tetradeoxy-D-*glycero*-D-*talo*-nonulosonic acid; 8-epi -legionaminic acid (8eLeg5Ac7Ac), 5,7-diacetamido-3,5,7,9-tetradeoxy-L-*glycero*-D-*galacto*-nonulosonic acid; acetyl-CoA, acetyl-coenzymeA; bacillosamine, 2,4-diamino-2,4,6-trideoxy-glucose; CDP, cytidine-5′-diphosphate; CE, capillary electrophoresis; CMP, cytidine-5′-monophosphate; CTP, cytidine-5′-triphosphate; diP, di-phosphate; DNA, deoxyribonucleic acid; DTT, dithiothreitol; EDTA, ethylenediaminetetraacetic acid; Fru, fructose; GalN, galactosamine; GDP, guanosine-5′-diphosphate; Glc, glucose; GlcN, glucosamine; GlcNAc, *N*-acetyl-glucosamine; Gln, glutamine; Glu, glutamate; GTP, guanosine-5′-triphosphate; HexNAc, *N*-acetyl-hexosamine; HSQC, heteronuclear single quantum coherence; legionaminic acid (Leg5Ac7Ac), 5,7-diacetamido-3,5,7,9-tetradeoxy-D-*glycero*-D-*galacto*-nonulosonic acid; Man, mannose; ManNAc, *N*-acetyl-mannosamine; MS, mass spectrometry; MS ring, the first flagellar basal body substructure located in the cytoplasmic membrane; NAD, nicotinamide adenine dinucleotide; NADP, nicotinamide adenine dinucleotide phosphate; NCAM, neural cell adhesion molecule; NDP, nucleotide diphosphate; Neu, neuraminic acid; NMR, nuclear magnetic resonance; NTP, nucleotide triphosphate; P, phosphate; PEP, phosphoenolpyruvate; P_i, inorganic phosphate; PP_i, pyrophosphate; PLP, pyridoxal-5′-phosphate; pseudaminic acid (Pse5Ac7Ac), 5,7-diacetamido-3,5,7,9-tetradeoxy-L-*glycero*-L-*manno*-nonulosonic acid; SDS–PAGE, sodium dodecyl sulfate—polyacrylamide gel electrophoresis; sialic acid (Neu5Ac), 5-acetamido-3,5-dideoxy-D-*glycero*-D-*galacto*-nonulosonic acid; TDP, thymidine-5′-diphosphate; TTP, thymidine-5′-triphosphate; UDP, uridine-5′-diphosphate.

References

Angström J, Teneberg S, Karlsson KA. 1994. Delineation and comparison of ganglioside-binding epitopes for the toxins of *Vibrio cholerae*, *Escherichia coli*, and *Clostridium tetani*: Evidence for overlapping epitopes. *Proc Natl Acad Sci USA*. 91:11859–11863.

Avril T, Wagner ER, Willison HJ, Crocker PR. 2006. Sialic acid-binding immunoglobulin-like lectin 7 mediates selective recognition of sialylated glycans expressed on *Campylobacter jejuni* lipooligosaccharides. *Infect Immun*. 74:4133–4141.

Bork K, Gagiannis D, Orthmann A, Weidemann W, Kontou M, Reutter W, Horstkorte R. 2007. Experimental approaches to interfere with the polysialylation of the neural cell adhesion molecule in vitro and in vivo. *J Neurochem*. 103:65–71.

Buse MG, Robinson KA, Marshall BA, Mueckler M. 1996. Differential effects of GLUT1 or GLUT4 overexpression on hexosamine biosynthesis by muscles of transgenic mice. *J Biol Chem*. 271:23197–23202.

Castric P, Cassels FJ, Carlson RW. 2001. Structural characterization of the *Pseudomonas aeruginosa* 1244 pilin glycan. *J Biol Chem*. 276:26479–26485.

Cazalet C, Jarraud S, Ghavi-Helm Y, Kunst F, Glaser P, Etienne J, Buchrieser C. 2008. Multigenome analysis identifies a worldwide distributed epidemic *Legionella pneumophila* clone that emerged within a highly diverse species. *Genome Res*. 18:431–441.

Crocker PR, Paulson JC, Varki A. 2007. Siglecs and their roles in the immune system. *Nat Rev Immunol*. 7:255–266.

Delputte PL, Van Breedam W, Delrue I, Oetke C, Crocker PR, Nauwynck HJ. 2007. Porcine arterivirus attachment to the macrophage-specific receptor sialoadhesin is dependent on the sialic acid-binding activity of the *N*-terminal immunoglobulin domain of sialoadhesin. *J Virol*. 81:9546–9550.

Fernandez-Moreira E, Helbig JH, Swanson MS. 2006. Membrane vesicles shed by *Legionella pneumophila* inhibit fusion of phagosomes with lysosomes. *Infect Immun*. 74:3285–3295.

Ginsburg V. 1978. Comparative biochemistry of nucleotide-linked sugars. *Prog Clin Biol Res*. 23:595–600.

Glaze PA, Watson DC, Young NM, Tanner ME. 2008. Biosynthesis of CMP-N,N′-diacetyllegionaminic acid from UDP-N,N′-diacetylbacillosamine in *Legionella pneumophila*. *Biochemistry*. 47:3272–3282.

Hausman SZ, Burns DL. 1993. Binding of pertussis toxin to lipid vesicles containing glycolipids. *Infect Immun*. 61:335–337.

Hedlund M, Ng E, Varki A, Varki NM. 2008. α2-6-Linked sialic acids on *N*-glycans modulate carcinoma differentiation in vivo. *Cancer Res*. 68:388–394.

Hsu KL, Pilobello KT, Mahal LK. 2006. Analyzing the dynamic bacterial glycome with a lectin microarray approach. *Nat Chem Biol*. 2:153–157.

Jolly L, Ferrari P, Blanot D, van Heijenoort J, Fassy F, Mengin-Lecreulx D. 1999. Reaction mechanism of phosphoglucosamine mutase from *Escherichia coli*. *Eur J Biochem*. 262:202–210.

Kiss E, Kereszt A, Barta F, Stephens S, Reuhs BL, Kondorosi A, Putnoky P. 2001. The rkp-3 gene region of *Sinorhizobium meliloti* RM41 contains strain-specific genes that determine K antigen structure. *Mol Plant Microbe Interact*. 14:1395–1403.

Knirel YA, Rietschel ET, Marre R, Zähringer U. 1994. The structure of the *O*-specific chain of *Legionella pneumophila* serogroup 1 lipopolysaccharide. *Eur J Biochem*. 221:239–245.

Knirel YA, Shashkov AS, Tsvetkov YE, Jansson PE, Zähringer U. 2003. 5,7-Diamino-3,5,7,9-tetradeoxynon-2-ulosonic acids in bacterial glycopolymers: Chemistry and biochemistry. *Adv Carbohydr Chem Biochem.* 58:371–417.

Kooistra O, Lüneberg E, Knirel YA, Frosch M, Zähringer U. 2002. *N*-Methylation in polylegionaminic acid is associated with the phase-variable epitope of *Legionella pneumophila serogroup* 1 lipopolysaccharide. Identification of 5-(*N*,*N*-dimethylacetimidoyl)amino and 5-acetimidoyl(*N*-methyl)amino-7-acetamido-3,5,7,9-tetradeoxynon-2-ulosonic acid in the *O*-chain polysaccharide. *Eur J Biochem*. 269:560–572.

Lehmann F, Tiralongo E, Tiralongo J. 2006. Sialic acid-specific lectins: Occurrence, specificity and function. *Cell Mol Life Sci*. 63:1331–1354.

Lundgren BR, Boddy CN. 2007. Sialic acid and *N*-acyl sialic acid analog production by fermentation of metabolically and genetically engineered *Escherichia coli*. *Org Biomol Chem*. 5:1903–1909.

Maki M, Renkonen R. 2004. Biosynthesis of 6-deoxyhexose glycans in bacteria. *Glycobiology*. 14:1R–15R.

McNally DJ, Aubry AJ, Hui JP, Khieu NH, Whitfield D, Ewing CP, Guerry P, Brisson J-R, Logan SM, Soo EC. 2007. Targeted metabolomics analysis of *Campylobacter coli* VC167 reveals legionaminic acid derivatives as novel flagellar glycans. *J Biol Chem*. 282:14463–14475.

Mengin-Lecreulx D, van Heijenoort J. 1994. Copurification of glucosamine-1-phosphate acetyltransferase and *N*-acetylglucosamine-1-phosphate uridyltransferase activities of *Escherichia coli*: Characterization of the *glmU* gene product as a bifunctional enzyme catalyzing two subsequent steps in the pathway for UDP-*N*-acetylglucosamine synthesis. *J Bacteriol*. 176:5788–5795.

Mengin-Lecreulx D, van Heijenoort J. 1996. Characterization of the essential gene *glmM* encoding phosphoglucosamine mutase in *Escherichia coli*. *J Biol Chem*. 271:32–39.

Merritt EA, Kuhn P, Sarfaty S, Erbe JL, Holmes RK, Hol WG. 1998. The 1.25 A resolution refinement of the cholera toxin B-pentamer: Evidence of peptide backbone strain at the receptor-binding site. *J Mol Biol*. 282:1043–1059.

Mouilleron S, Badet-Denisot MA, Golinelli-Pimpaneau B. 2006. Glutamine binding opens the ammonia channel and activates glucosamine-6P synthase. *J Biol Chem*. 281:4404–4412.

Nikaido H, Nikaido K, Makela PH. 1966. Genetic determination of enzymes synthesizing *O*-specific sugars of *Salmonella* lipopolysaccharides. *J Bacteriol*. 91:1126–1135.

Olivier NB, Chen MM, Behr JR, Imperiali B. 2006. In vitro biosynthesis of UDP-N,N′-diacetylbacillosamine by enzymes of the *Campylobacter jejuni* general protein glycosylation system. *Biochemistry*. 45:13659–13669.

Pompeo F, Bourne Y, van Heijenoort J, Fassy F, Mengin-Lecreulx D. 2001. Dissection of the bifunctional *Escherichia coli N*-acetylglucosamine-1-phosphate uridyltransferase enzyme into autonomously functional domains and evidence that trimerization is absolutely required for glucosamine-1-phosphate acetyltransferase activity and cell growth. *J Biol Chem*. 276:3833–3839.

Pontes de Carvalho LC, Tomlinson S, Vandekerckhove F, Bienen EJ, Clarkson AB, Jiang MS, Hart GW, Nussenzweig V. 1993. Characterization of a novel trans-sialidase of *Trypanosoma brucei* procyclic trypomastigotes and identification of procyclin as the main sialic acid acceptor. *J Exp Med*. 177:465–474.

Schirm M, Soo EC, Aubry AJ, Austin J, Thibault P, Logan SM. 2003. Structural, genetic and functional characterization of the flagellin glycosylation process in *Helicobacter pylori*. *Mol Microbiol*. 48:1579–1592.

Schoenhofen IC, Lunin VV, Julien JP, Li Y, Ajamian E, Matte A, Cygler M, Brisson J-R, Aubry A, Logan SM, et al. 2006. Structural and functional characterization of PseC, an aminotransferase involved in the biosynthesis of pseudaminic acid, an essential flagellar modification in *Helicobacter pylori*. *J Biol Chem*. 281:8907–8916.

Schoenhofen IC, McNally DJ, Brisson JR, Logan SM. 2006. Elucidation of the CMP-pseudaminic acid pathway in *Helicobacter pylori*: Synthesis from UDP-*N*-acetylglucosamine by a single enzymatic reaction. *Glycobiology*. 16:8C–14C.

Schoenhofen IC, McNally DJ, Vinogradov E, Whitfield D, Young NM, Dick S, Wakarchuk WW, Brisson J-R, Logan SM. 2006. Functional characterization of dehydratase/aminotransferase pairs from *Helicobacter* and *Campylobacter*: Enzymes distinguishing the pseudaminic acid and bacillosamine biosynthetic pathways. *J Biol Chem*. 281:723–732.

Severi E, Hood DW, Thomas, GH. 2007. Sialic acid utilization by bacterial pathogens. *Microbiology*. 153:2817–2822.

Silva E, Marques AR, Fialho AM, Granja AT, Sá-Correia I. 2005. Proteins encoded by *Sphingomonas elodea* ATCC 31461 *rmlA* and *ugpG* genes, involved in gellan gum biosynthesis, exhibit both dTDP- and UDP-glucose pyrophosphorylase activities. *Appl Environ Microbiol*. 71:4703–4712.

Stein PE, Boodhoo A, Armstrong GD, Heerze LD, Cockle SA, Klein MH, Read RJ. 1994. Structure of a pertussis toxin-sugar complex as a model for receptor binding. *Nat Struct Biol.* 1:591–596.

Teplyakov A, Obmolova G, Badet-Denisot MA, Badet B. 1999. The mechanism of sugar phosphate isomerization by glucosamine 6-phosphate synthase. *Protein Sci*. 8:596–602.

Thibault, P, Logan SM, Kelly JF, Brisson J-R, Ewing CP, Trust TJ, Guerry P. 2001. Identification of the carbohydrate moieties and glycosylation motifs in *Campylobacter jejuni* flagellin. *J Biol Chem*. 276:34862–34870.

Tsvetkov YE, Shashkov AS, Knirel YA, Zähringer U. 2001. Synthesis and identification in bacterial lipopolysaccharides of 5,7-diacetamido-3,5,7,9-tetradeoxy-D-*glycero*-D-*galacto*- and -D-*glycero*-D-*talo*-non-2-ulosonic acids. *Carbohydr Res*. 331:233–237.

Varki A. 2007. Glycan-based interactions involving vertebrate sialic-acid-recognizing proteins. *Nature*. 446:1023–1029.

Varki A, Angata T. 2006. Siglecs – the major subfamily of I-type lectins. *Glycobiology*. 16:1R–27R.

Varki NM, Varki A. 2007. Diversity in cell surface sialic acid presentations: Implications for biology and disease. *Lab Invest*. 87:851–857.

Yu VL, Plouffe JF, Pastoris MC, Stout JE, Schousboe M, Widmer A, Summersgill J, File T, Heath CM, Paterson DL, et al. 2002. Distribution of *Legionella species* and serogroups isolated by culture in patients with sporadic community-acquired legionellosis: An international collaborative survey. *J Infect Dis*. 186:127–128.